

## The dark matter: DAMA/LIBRA and its perspectives

R. Bernabei, P. Belli\*, V. Caracciolo, R. Cerulli and V. Merlo

*Dip. Fisica, Università di Roma "Tor Vergata",  
00133 Rome, Italy*

*INFN sezione di Roma "Tor Vergata", 00133 Rome, Italy*

*\*E-mail: pierluigi.belli@roma2.infn.it*

F. Cappella, A. d'Angelo and A. Incicchitti

*Dip. Fisica, Università di Roma "La Sapienza",  
00185 Rome, Italy*

*INFN sezione di Roma, 00185 Rome, Italy*

C.J. Dai, X.H. Ma and X.D. Sheng

*Key Laboratory of Particle Astrophysics, Institute of High Energy Physics,  
Chinese Academy of Sciences, 100049 Beijing, PR China*

F. Montecchia

*INFN sezione di Roma "Tor Vergata", 00133 Rome, Italy*

*Dip. Ingegneria Civile e Ingegneria Informatica, Università di Roma "Tor Vergata",  
00133 Rome, Italy*

Z.P. Ye

*Key Laboratory of Particle Astrophysics, Institute of High Energy Physics,  
Chinese Academy of Sciences, 100049 Beijing, PR China  
University of Jिंगgangshan, Ji'an, Jiangxi, PR China*

Experimental observations and theoretical arguments point out that Dark Matter (DM) particles are one of the most prominent component of the Universe. This motivated the pioneer DAMA experiment to investigate the presence of these particles in the galactic halo, by exploiting the model independent signature of the DM annual modulation of the rate and very highly radio-pure apparatus in underground site. In this paper the results obtained by other two annual cycles of DAMA/LIBRA-phase2 are presented and the long-standing model-independent annual modulation effect measured by DAMA deep underground at the Gran Sasso National Laboratory (LNGS) of the I.N.F.N. with different experimental configurations is summarized. In particular, the DAMA/LIBRA-phase2 apparatus,  $\simeq 250$  kg highly radio-pure NaI(Tl), profits from a second generation high quantum efficiency photomultipliers and of new electronics with respect to DAMA/LIBRA-phase1. The improved experimental configuration has also allowed to lower the software energy threshold. Including the results of these other two annual cycles presented here, the total exposure of DAMA/LIBRA-phase2 over 8 annual cycles is  $1.53 \text{ ton} \times \text{yr}$ . DAMA/LIBRA-phase2 confirms the evidence of a signal that meets all the requirements of the model independent Dark Matter annual modulation signature, at  $11.8 \sigma$  C.L. in the energy region (1–6) keV. In the energy region between 2 and 6 keV, where data are also available from DAMA/NaI and DAMA/LIBRA-phase1 (14 additional annual cycles), the achieved C.L. for the full exposure ( $2.86 \text{ ton} \times \text{yr}$ ) is  $13.7 \sigma$ ; the modulation amplitude of the *single-hit* scintillation events is:  $(0.01014 \pm 0.00074) \text{ cpd/kg/keV}$ ,

the measured phase is  $(142.4 \pm 4.2)$  days and the measured period is  $(0.99834 \pm 0.00067)$  yr, all these values are well in agreement with those expected for DM particles. No systematics or side reaction able to mimic the exploited DM signature (i.e. to account for the whole measured modulation amplitude and to simultaneously satisfy all the requirements of the signature), has been found or suggested by anyone throughout some decades thus far.

*Keywords:* Scintillation detectors; elementary particle processes; Dark Matter; annual modulation.

## 1. Introduction

The DAMA/LIBRA<sup>1-23</sup> experiment, as the pioneer DAMA/NaI<sup>24-51</sup>, has the main aim to investigate the presence of DM particles in the galactic halo by exploiting the DM annual modulation signature (originally suggested in Ref.<sup>52,53</sup>). In addition, the developed highly radio-pure NaI(Tl) target-detectors<sup>1,6,9,54</sup> ensure sensitivity to a wide range of DM candidates, interaction types and astrophysical scenarios (see e.g. Refs.<sup>2,14,16-18,25-32,35-42</sup>, and in literature).

The origin of the DM annual modulation signature and of its peculiar features is due to the Earth motion with respect to the DM particles constituting the Galactic Dark Halo. In fact, as a consequence of the Earth's revolution around the Sun, which is moving in the Galaxy with respect to the Local Standard of Rest towards the star Vega near the constellation of Hercules, the Earth should be crossed by a larger flux of DM particles around  $\simeq 2$  June and by a smaller one around  $\simeq 2$  December. In the former case the Earth orbital velocity is summed to that of the solar system with respect to the Galaxy, while in the latter the two velocities are subtracted. The DM annual modulation signature is very distinctive since the effect induced by DM particles must simultaneously satisfy all the following requirements: the rate must contain a component modulated according to a cosine function (1) with one year period (2) and a phase that peaks roughly  $\simeq 2$  June (3); this modulation must only be found in a well-defined low energy range, where DM particle induced events can be present (4); it must apply only to those events in which just one detector of many actually "fires" (*single-hit* events), since the DM particle multi-interaction probability is negligible (5); the modulation amplitude in the region of maximal sensitivity must be  $\lesssim 7\%$  of the constant part of the signal for usually adopted halo distributions (6), but it can be larger in case of some proposed scenarios such as e.g. those in Ref.<sup>55-59</sup> (even up to  $\simeq 30\%$ ). Thus this signature has many peculiarities and, in addition, it allows to test a wide range of parameters in many possible astrophysical, nuclear and particle physics scenarios.

This DM signature might be mimicked only by systematic effects or side reactions able to account for the whole observed modulation amplitude and to simultaneously satisfy all the requirements given above.

The full description of the DAMA/LIBRA set-up and the adopted procedures during the phase1 and phase2 and other related arguments have been discussed in details e.g. in Refs.<sup>1-6,19-21,23</sup>.

At the end of 2010 all the photomultipliers (PMTs) were replaced by a second generation PMTs Hamamatsu R6233MOD, with higher quantum efficiency (Q.E.) and with lower background with respect to those used in phase1; they were produced after a dedicated R&D in the company, and tests and selections<sup>6,54</sup>. The new PMTs have Q.E. in the range 33-39% at 420 nm, wavelength of NaI(Tl) emission, and in the range 36-44% at peak. The commissioning of the DAMA/LIBRA-phase2 experiment was successfully performed in 2011, allowing the achievement of the software energy threshold at 1 keV, and the improvement of some detector's features such as energy resolution and acceptance efficiency near software energy threshold<sup>6</sup>.

The adopted procedure for noise rejection near software energy threshold and the acceptance windows are the same unchanged along all the DAMA/LIBRA-phase2 data taking, throughout the months and the annual cycles. The typical behaviour of the overall efficiency for *single-hit* events as a function of the energy is also shown in Ref.<sup>6</sup>; the percentage variations of the efficiency follow a gaussian distribution with  $\sigma = 0.3\%$  and do not show any modulation with period and phase as expected for the DM signal (for a partial data release see Ref.<sup>21</sup>).

At the end of 2012 new preamplifiers and special developed trigger modules were installed and the apparatus was equipped with more compact electronic modules<sup>60</sup>. Here we just remind that the sensitive part of DAMA/LIBRA-phase2 set-up is made of 25 highly radio-pure NaI(Tl) crystal scintillators (5-rows by 5-columns matrix) having 9.70 kg mass each one; quantitative analyses of residual contaminants are given in Ref.<sup>1</sup>. In each detector two 10 cm long UV light guides (made of Suprasil B quartz) act also as optical windows on the two end faces of the crystal, and are coupled to two low background PMTs working in coincidence at single photoelectron level. The detectors are housed in a sealed low-radioactive copper box installed in the center of a low-radioactive Cu/Pb/Cd-foils/polyethylene/paraffin shield; moreover, about 1 m concrete (made from the Gran Sasso rock material) almost fully surrounds (mostly outside the barrack) this passive shield, acting as a further neutron moderator. The shield is decoupled from the ground by a metallic structure mounted above a concrete basement; a neoprene layer separates the concrete basement and the floor of the laboratory. The space between this basement and the metallic structure is filled by paraffin for several tens cm in height.

A threefold-level sealing system prevents the detectors from contact with the environmental air of the underground laboratory and continuously maintains them in HP (high-purity) Nitrogen atmosphere. The whole installation is under air conditioning to ensure a suitable and stable working temperature. The huge heat capacity of the multi-tons passive shield ( $\approx 10^6$  cal/ $^{\circ}$ C) guarantees further relevant stability of the detectors' operating temperature. In particular, two independent systems of air conditioning are available for redundancy: one cooled by water refrigerated by a dedicated chiller and the other operating with cooling gas. A hardware/software monitoring system provides data on the operating conditions. In particular, several probes are read out and the results are stored with the production

data. Moreover, self-controlled computer based processes automatically monitor several parameters, including those from DAQ, and manage the alarms system. All these procedures, already experienced during DAMA/LIBRA-phase1<sup>1-5</sup>, allow us to control and to maintain the running conditions stable at a level better than 1% also in DAMA/LIBRA-phase2 (see e.g. Ref.<sup>21,23</sup>).

The light response of the detectors during phase2 typically ranges from 6 to 10 photoelectrons/keV, depending on the detector. Energy calibration with X-rays/ $\gamma$  sources are regularly carried out in the same running condition down to few keV (for details see e.g. Ref.<sup>1</sup>; in particular, double coincidences due to internal X-rays from <sup>40</sup>K (which is at ppt levels in the crystals) provide (when summing the data over long periods) a calibration point at 3.2 keV close to the software energy threshold. The DAQ system records both *single-hit* events (where just one of the detectors fires) and *multiple-hit* events (where more than one detector fires) up to the MeV region despite the optimization is performed for the lowest energy.

The radio-purity and details are discussed e.g. in Refs.<sup>1-5,54</sup> and references therein. The adopted procedures provide sensitivity to large and low mass DM candidates inducing nuclear recoils and/or electromagnetic signals.

The data of the former DAMA/NaI setup and, later, those of the DAMA/LIBRA-phase1 have already given (with high confidence level) positive evidence for the presence of a signal that satisfies all the requirements of the exploited DM annual modulation signature<sup>2-5,35,36</sup>.

In this paper the model independent result of eight annual cycles of DAMA/LIBRA-phase2 is presented. The total exposure of DAMA/LIBRA-phase2 is: 1.53 ton  $\times$  yr with an energy threshold at 1 keV; when including also that of the first generation DAMA/NaI experiment and DAMA/LIBRA-phase1 the cumulative exposure is 2.86 ton  $\times$  yr, corresponding to twenty-two independent annual cycles.

## 2. The DAMA/LIBRA-phase2 annual cycles

The details of the annual cycles of DAMA/LIBRA-phase2 are reported in Table 1. The first annual cycle was dedicated to the commissioning and to the optimizations towards the achievement of the 1 keV software energy threshold<sup>6</sup>. This period has: i) no data before/near Dec. 2, 2010 (the expected minimum of the DM signal); ii) data sets with some set-up modifications; iii)  $(\alpha - \beta^2) = 0.355$  well different from 0.5 (i.e. the detectors were not being operational evenly throughout the year). Thus, this period cannot be used for the annual modulation studies; however, it has been used for other purposes<sup>6,13</sup>. Therefore, as shown in Table 1 the considered annual cycles of DAMA/LIBRA-phase2 are eight (exposure of 1.53 ton $\times$ yr). The cumulative exposure, also considering the former DAMA/NaI and DAMA/LIBRA-phase1, is 2.86 ton $\times$ yr.

The total number of events collected for the energy calibrations during the eight annual cycles of DAMA/LIBRA-phase2 is about  $1.6 \times 10^8$ , while about  $1.7 \times 10^5$

Table 1. Details about the annual cycles of DAMA/LIBRA–phase2. The mean value of the squared cosine is  $\alpha = \langle \cos^2 \omega(t - t_0) \rangle$  and the mean value of the cosine is  $\beta = \langle \cos \omega(t - t_0) \rangle$  (the averages are taken over the live time of the data taking and  $t_0 = 152.5$  day, i.e. June 2<sup>nd</sup>); thus, the variance of the cosine,  $(\alpha - \beta^2)$ , is  $\simeq 0.5$  for a detector being operational evenly throughout the year.

DAMA/LIBRA–phase2 annual cycle	Period	Mass (kg)	Exposure (kg×day)	$(\alpha - \beta^2)$
1	Dec. 23, 2010 – Sept. 9, 2011		commissioning of phase2	
2	Nov. 2, 2011 – Sept. 11, 2012	242.5	62917	0.519
3	Oct. 8, 2012 – Sept. 2, 2013	242.5	60586	0.534
4	Sept. 8, 2013 – Sept. 1, 2014	242.5	73792	0.479
5	Sept. 1, 2014 – Sept. 9, 2015	242.5	71180	0.486
6	Sept. 10, 2015 – Aug. 24, 2016	242.5	67527	0.522
7	Sept. 7, 2016 – Sept. 25, 2017	242.5	75135	0.480
8	Sept. 25, 2017 – Aug. 20, 2018	242.5	68759	0.557
9	Aug. 24, 2018 – Oct. 3, 2019	242.5	77213	0.446
DAMA/LIBRA–phase2	Nov. 2, 2011 – Oct. 3, 2019	557109 kg×day $\simeq$ 1.53 ton×yr		0.501
DAMA/NaI + DAMA/LIBRA–phase1 + DAMA/LIBRA–phase2:			2.86 ton×yr	

events/keV have been collected for the evaluation of the acceptance window efficiency for noise rejection near the software energy threshold<sup>1,6</sup>.

As it can be inferred from Table 1, the duty cycle of the experiment is high, ranging between 76% and 86%. The routine calibrations and, in particular, the data collection for the acceptance windows efficiency mainly affect it.

### 3. The annual modulation of the residual rate

Fig. 1 shows the time behaviour of the experimental residual rates of the *single-hit* scintillation events in the (1–3), and (1–6) keV energy intervals for DAMA/LIBRA–phase2. The residual rates are calculated from the measured rate of the *single-hit* events after subtracting the constant part, as described in Refs.<sup>2–5,35,36</sup>. The null modulation hypothesis is rejected at very high C.L. by  $\chi^2$  test:  $\chi^2 = 176$  and 202, respectively, over 69 d.o.f.. The P-values are  $P = 2.6 \times 10^{-11}$ , and  $P = 5.6 \times 10^{-15}$ , respectively. The residuals of the DAMA/NaI data (0.29 ton × yr) are given in Ref.<sup>2,5,35,36</sup>, while those of DAMA/LIBRA–phase1 (1.04 ton × yr) in Ref.<sup>2–5</sup>.

The former DAMA/LIBRA–phase1 and the new DAMA/LIBRA–phase2 residual rates of the *single-hit* scintillation events are reported in Fig. 2. The energy interval is from 2 keV, the software energy threshold of DAMA/LIBRA–phase1, up to 6 keV. The null modulation hypothesis is rejected at very high C.L. by  $\chi^2$  test:  $\chi^2/d.o.f. = 240/119$ , corresponding to P-value =  $3.5 \times 10^{-10}$ .

The *single-hit* residual rates of the DAMA/LIBRA–phase2 (Fig. 1) have been fitted with the function:  $A \cos \omega(t - t_0)$ , considering a period  $T = \frac{2\pi}{\omega} = 1$  yr and a phase  $t_0 = 152.5$  day (June 2<sup>nd</sup>) as expected by the DM annual modulation signature; this can be repeated for the only case of (2–6) keV energy interval also including the former DAMA/NaI and DAMA/LIBRA–phase1 data. The goodness of the fits

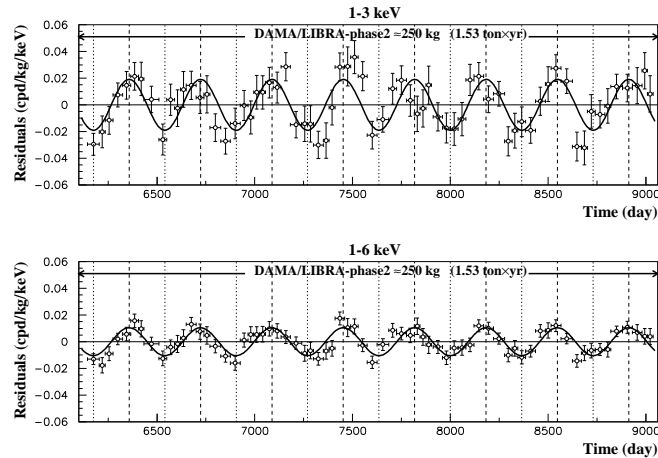


Fig. 1. Experimental residual rate of the *single-hit* scintillation events measured by DAMA/LIBRA-phase2 over eight annual cycles in the (1–3), and (1–6) keV energy intervals as a function of the time. The time scale is maintained the same of the previous DAMA papers for consistency. The data points present the experimental errors as vertical bars and the associated time bin width as horizontal bars. The superimposed curves are the cosinusoidal functional forms  $A \cos \omega(t - t_0)$  with a period  $T = \frac{2\pi}{\omega} = 1$  yr, a phase  $t_0 = 152.5$  day (June 2<sup>nd</sup>) and modulation amplitudes,  $A$ , equal to the central values obtained by best fit on the data points of the entire DAMA/LIBRA-phase2. The dashed vertical lines correspond to the maximum expected for the DM signal (June 2<sup>nd</sup>), while the dotted vertical lines correspond to the minimum.

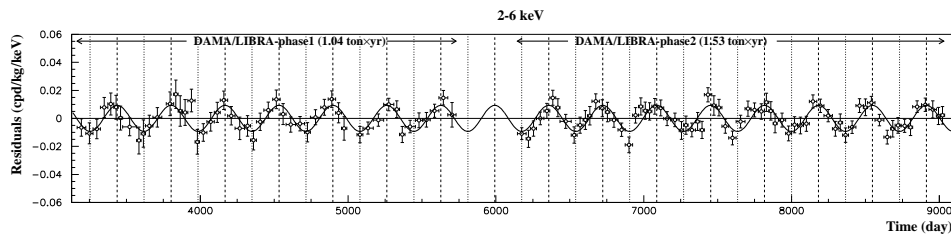


Fig. 2. Experimental residual rate of the *single-hit* scintillation events measured by DAMA/LIBRA-phase1 and DAMA/LIBRA-phase2 in the (2–6) keV energy intervals as a function of the time. The superimposed curve is the cosinusoidal functional forms  $A \cos \omega(t - t_0)$  with a period  $T = \frac{2\pi}{\omega} = 1$  yr, a phase  $t_0 = 152.5$  day (June 2<sup>nd</sup>) and modulation amplitude,  $A$ , equal to the central value obtained by best fit on the data points of DAMA/LIBRA-phase1 and DAMA/LIBRA-phase2. For details see Fig. 1.

is well supported by the  $\chi^2$  test; for example,  $\chi^2/d.o.f. = 81.6/68, 66.2/68, 130/155$  are obtained for the (1–3) keV and (1–6) keV cases of DAMA/LIBRA-phase2, and for the (2–6) keV case of DAMA/NaI, DAMA/LIBRA-phase1 and DAMA/LIBRA-phase2, respectively. The results of the best fits in the different cases are summarized in Table 2. Table 2 also reports the cases when the period and the phase are kept free in the fitting procedure. The period and the phase are well compatible with expectations for a DM annual modulation signal. In particular, the phase is consistent with about June 2<sup>nd</sup> and is fully consistent with the value indepen-

Table 2. Modulation amplitude,  $A$ , obtained by fitting the *single-hit* residual rate of DAMA/LIBRA–phase2, as reported in Fig. 1, and also including the residual rates of the former DAMA/NaI and DAMA/LIBRA–phase1. It was obtained by fitting the data with the formula:  $A \cos \omega(t - t_0)$ . The period  $T = \frac{2\pi}{\omega}$  and the phase  $t_0$  are kept fixed at 1 yr and at 152.5 day (June 2<sup>nd</sup>), respectively, as expected by the DM annual modulation signature, and alternatively kept free. The results are well compatible with expectations for a signal in the DM annual modulation signature.

	$A$ (cpd/kg/keV)	$T = \frac{2\pi}{\omega}$ (yr)	$t_0$ (days)	C.L.
DAMA/LIBRA–phase2:				
1-3 keV	(0.0191±0.0020)	1.0	152.5	9.7 $\sigma$
1-6 keV	(0.01048±0.00090)	1.0	152.5	11.6 $\sigma$
2-6 keV	(0.00933±0.00094)	1.0	152.5	9.9 $\sigma$
1-3 keV	(0.0191±0.0020)	(0.99952±0.00080)	149.6±5.9	9.6 $\sigma$
1-6 keV	(0.01058±0.00090)	(0.99882±0.00065)	144.5±5.1	11.8 $\sigma$
2-6 keV	(0.00954±0.00076)	(0.99836±0.00075)	141.1±5.9	12.6 $\sigma$
DAMA/LIBRA–phase1 + phase2:				
2-6 keV	(0.00941±0.00076)	1.0	152.5	12.4 $\sigma$
2-6 keV	(0.00959±0.00076)	(0.99835±0.00069)	142.0±4.5	12.6 $\sigma$
DAMA/NaI + DAMA/LIBRA–phase1 + phase2:				
2-6 keV	(0.00996±0.00074)	1.0	152.5	13.4 $\sigma$
2-6 keV	(0.01014±0.00074)	(0.99834±0.00067)	142.4±4.2	13.7 $\sigma$

dently determined by Maximum Likelihood analysis (see later). For completeness, we recall that a slight energy dependence of the phase could be expected (see e.g. Refs. <sup>38,58,59,61–63</sup>), providing intriguing information on the nature of Dark Matter candidate and related aspects.

#### 4. Absence of modulation of the background

As done in previous data releases, absence of any significant background modulation in the energy spectrum has also been verified in the present data taking for energy regions not of interest for DM. In fact, the background in the lowest energy region is essentially due to “Compton” electrons, X-rays and/or Auger electrons, muon induced events, etc., which are strictly correlated with the events in the higher energy region of the spectrum. Thus, if a modulation detected in the lowest energy region were due to a modulation of the background (rather than to a signal), an equal or larger modulation in the higher energy regions should be present.

For example, the measured rate integrated above 90 keV,  $R_{90}$ , as a function of the time has been analysed. Fig. 3 shows the distribution of the percentage variations of  $R_{90}$  with respect to the mean values for all the detectors in DAMA/LIBRA–phase2. It shows a cumulative gaussian behaviour with  $\sigma \simeq 1\%$ , well accounted for by the statistical spread expected from the used sampling time.

Moreover, fitting the time behaviour of  $R_{90}$  including a term with phase and period as for DM particles, a modulation amplitude  $A_{R_{90}}$  compatible with zero has been found for all the annual cycles (see Table 3). This also excludes the presence of

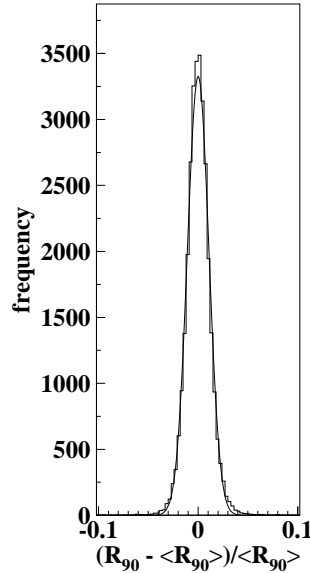


Fig. 3. Distribution of the percentage variations of  $R_{90}$  with respect to the mean values for all the detectors in the DAMA/LIBRA-phase2 (histogram); the superimposed curve is a gaussian fit.

any background modulation in the whole energy spectrum at a level much lower than the effect found in the lowest energy region for the *single-hit* scintillation events. In fact, otherwise – considering the  $R_{90}$  mean values – a modulation amplitude of order of tens cpd/kg would be present for each annual cycle, that is  $\simeq 100 \sigma$  far away from the measured values.

Table 3. Modulation amplitudes,  $A_{R_{90}}$ , obtained by fitting the time behaviour of  $R_{90}$  in DAMA/LIBRA-phase2, including a term with a cosine function having phase and period as expected for a DM signal. The obtained amplitudes are compatible with zero, and incompatible ( $\simeq 100 \sigma$ ) with modulation amplitudes of tens cpd/kg. Modulation amplitudes,  $A_{(6-14)}$ , obtained by fitting the time behaviour of the residual rates of the *single-hit* scintillation events in the (6–14) keV energy interval. In the fit the phase and the period are at the values expected for a DM signal. The obtained amplitudes are compatible with zero.

DAMA/LIBRA-phase2 annual cycle	$A_{R_{90}}$ (cpd/kg)	$A_{(6-14)}$ (cpd/kg/keV)
2	$(0.12 \pm 0.14)$	$(0.0032 \pm 0.0017)$
3	$-(0.08 \pm 0.14)$	$(0.0016 \pm 0.0017)$
4	$(0.07 \pm 0.15)$	$(0.0024 \pm 0.0015)$
5	$-(0.05 \pm 0.14)$	$-(0.0004 \pm 0.0015)$
6	$(0.03 \pm 0.13)$	$(0.0001 \pm 0.0015)$
7	$-(0.09 \pm 0.14)$	$(0.0015 \pm 0.0014)$
8	$-(0.18 \pm 0.13)$	$-(0.0005 \pm 0.0013)$
9	$(0.08 \pm 0.14)$	$-(0.0003 \pm 0.0014)$

Similar results are obtained when comparing the *single-hit* residuals in the



(1–6) keV with those in other energy intervals; for example Fig. 4 shows the *single-hit* residuals in the (1–6) keV and in the (10–20) keV energy regions for DAMA/LIBRA–phase2 as if they were collected in a single annual cycle (i.e. binning in the variable time from the January 1st of each annual cycle).

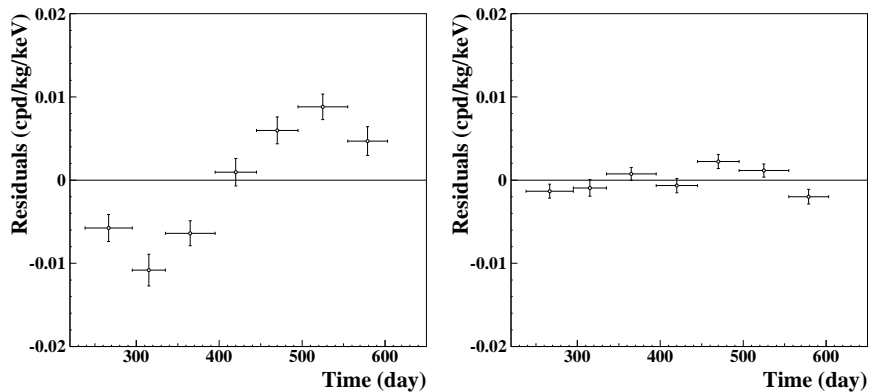


Fig. 4. Experimental *single-hit* residuals in the (1–6) keV and in the (10–20) keV energy regions for DAMA/LIBRA–phase2 as if they were collected in a single annual cycle (i.e. binning in the variable time from the January 1st of each annual cycle). The data points present the experimental errors as vertical bars and the associated time bin width as horizontal bars. The initial time of the figures is taken at August 7<sup>th</sup>. A clear modulation satisfying all the peculiarities of the DM annual modulation signature is present in the lowest energy interval with  $A=(0.00956 \pm 0.00090)$  cpd/kg/keV, while it is absent just above:  $A=(0.0007 \pm 0.0005)$  cpd/kg/keV.

Moreover, Table 3 shows the modulation amplitudes obtained by fitting the time behaviour of the residual rates of the *single-hit* scintillation events in the (6–14) keV energy interval for the DAMA/LIBRA–phase2 annual cycles. In the fit the phase and the period are at the values expected for a DM signal. The obtained amplitudes are compatible with zero.

A further relevant investigation on DAMA/LIBRA–phase2 data has been performed by applying the same hardware and software procedures, used to acquire and to analyse the *single-hit* residual rate, to the *multiple-hit* one. Since the probability that a DM particle interacts in more than one detector is negligible, a DM signal can be present just in the *single-hit* residual rate. Thus, the comparison of the results of the *single-hit* events with those of the *multiple-hit* ones corresponds to compare the cases of DM particles beam-on and beam-off. This procedure also allows an additional test of the background behaviour in the same energy interval where the positive effect is observed.

In particular, in Fig. 5 the residual rates of the *single-hit* scintillation events collected during DAMA/LIBRA–phase2 are reported, as collected in a single cycle, together with the residual rates of the *multiple-hit* events, in the considered energy intervals. While, as already observed, a clear modulation, satisfying all the peculiarities of the DM annual modulation signature, is present in the *single-hit* events,

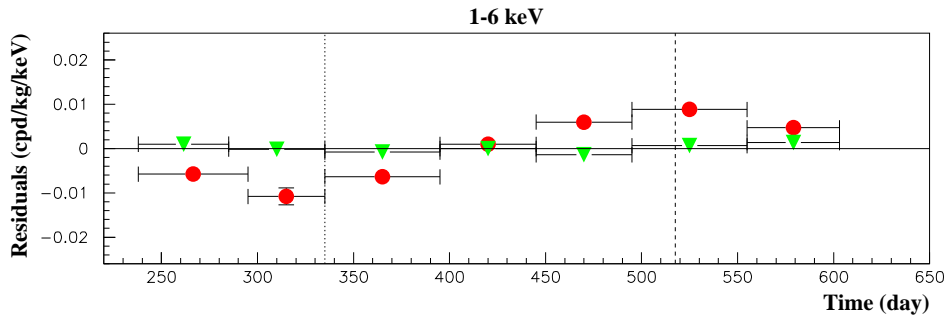


Fig. 5. Experimental residual rates of DAMA/LIBRA–phase2 *single-hit* events (filled red on-line circles), class of events to which DM events belong, and for *multiple-hit* events (filled green on-line triangles), class of events to which DM events do not belong. They have been obtained by considering for each class of events the data as collected in a single annual cycle and by using in both cases the same identical hardware and the same identical software procedures. The initial time of the figure is taken on August 7<sup>th</sup>. The experimental points present the errors as vertical bars and the associated time bin width as horizontal bars. Analogous results were obtained for DAMA/NaI (two last annual cycles) and DAMA/LIBRA–phase1<sup>2–5,36</sup>.

the fitted modulation amplitude for the *multiple-hit* residual rate is well compatible with zero:  $(0.00030 \pm 0.00032)$  cpd/kg/keV in the (1–6) keV energy region. Thus, again evidence of annual modulation with proper features as required by the DM annual modulation signature is present in the *single-hit* residuals (events class to which the DM particle induced events belong), while it is absent in the *multiple-hit* residual rate (event class to which only background events belong). Similar results were also obtained for the two last annual cycles of DAMA/NaI<sup>36</sup> and for DAMA/LIBRA–phase1<sup>2–5</sup>. Since the same identical hardware and the same identical software procedures have been used to analyse the two classes of events, the obtained result offers an additional strong support for the presence of a DM particle component in the galactic halo.

In conclusion, no background process able to mimic the DM annual modulation signature (that is, able to simultaneously satisfy all the peculiarities of the signature and to account for the measured modulation amplitude) has been found or suggested by anyone throughout some decades thus far (see also discussions e.g. in Ref. <sup>1–5,7,8,19–21,23,34–36</sup>).

## 5. The analysis in frequency

To perform the Fourier analysis of the DAMA/LIBRA–phase1 and phase2 data in a wider region of considered frequency, the *single-hit* events have been grouped in 1 day bins. Due to the low statistics in each time bin, a procedure detailed in Ref. <sup>64</sup> has been followed. The whole power spectra up to the Nyquist frequency and the zoomed ones are reported in Fig. 6. A clear peak corresponding to a period of 1 year is evident for the lowest energy interval; the same analysis in the (6–14) keV

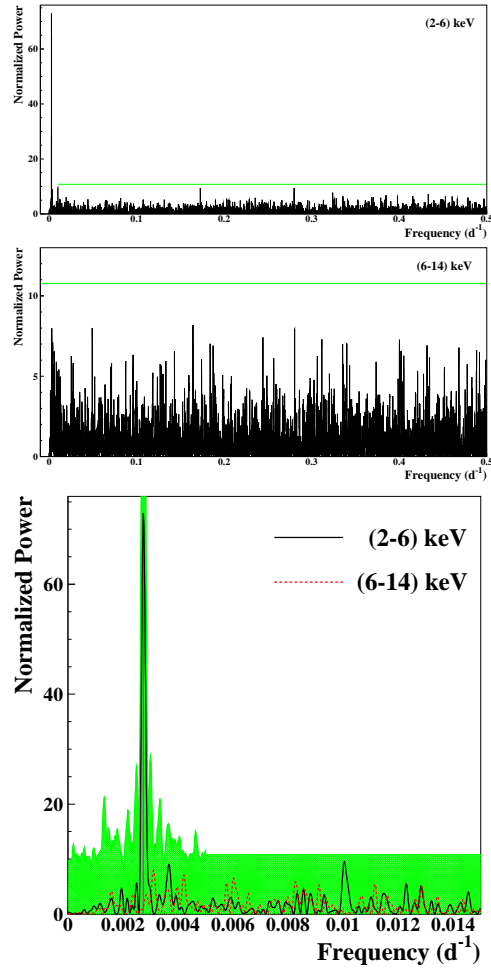


Fig. 6. Power spectra of the time sequence of the measured *single-hit* events for DAMA/LIBRA–phase1 and DAMA/LIBRA–phase2 grouped in 1 day bins. From top to bottom: spectra up to the Nyquist frequency for (2–6) keV and (6–14) keV energy intervals and their zoom around the  $1 \text{ y}^{-1}$  peak, for (2–6) keV (solid line) and (6–14) keV (dotted line) energy intervals. The main mode present at the lowest energy interval corresponds to a frequency of  $2.74 \times 10^{-3} \text{ d}^{-1}$  (vertical line, purple on-line). It corresponds to a period of  $\simeq 1$  year. A similar peak is not present in the (6–14) keV energy interval. The shaded (green on-line) area in the bottom figure – calculated by Monte Carlo procedure – represents the 90% C.L. region where all the peaks are expected to fall for the (2–6) keV energy interval. In the frequency range far from the signal for the (2–6) keV energy region and for the whole (6–14) keV spectrum, the upper limit of the shaded region (90% C.L.) can be calculated to be 10.8 (continuous lines, green on-line).

energy region shows only aliasing peaks instead. Neither other structure at different frequencies has been observed.

As to the significance of the peaks present in the periodogram, we remind that the periodogram ordinate,  $z$ , at each frequency follows a simple exponential distribution  $e^{-z}$  in the case of the null hypothesis or white noise<sup>65</sup>. Therefore, if  $M$

independent frequencies are scanned, the probability to obtain values larger than  $z$  is:  $P(> z) = 1 - (1 - e^{-z})^M$ .

In general  $M$  depends on the number of sampled frequencies, the number of data points  $N$ , and their detailed spacing. It turns out that  $M$  is very nearly equal to  $N$  when the data points are approximately equally spaced, and when the sampled frequencies cover the frequency range from 0 to the Nyquist frequency<sup>66,67</sup>.

The number of data points used to obtain the spectra in Fig. 6 is  $N = 5047$  (days measured over the 5479 days of the 15 DAMA/LIBRA–phase1 and phase2 annual cycles) and the full frequencies region up to Nyquist frequency has been scanned. Therefore, assuming  $M = N$ , the significance levels  $P = 0.10$ ,  $0.05$  and  $0.01$ , correspond to peaks with heights larger than  $z = 10.8$ ,  $11.5$  and  $13.1$ , respectively, in the spectra of Fig 6.

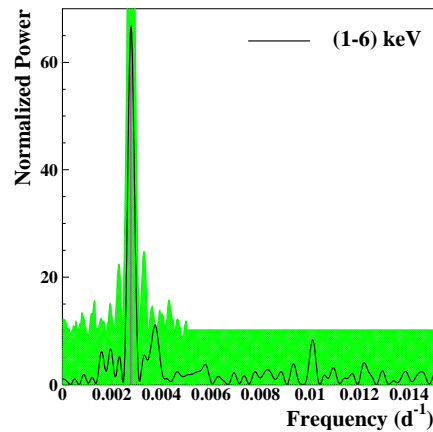


Fig. 7. Power spectrum of the time sequence of the measured *single-hit* events in the (1–6) keV energy interval for DAMA/LIBRA–phase2 grouped in 1 day bin. The main mode present at the lowest energy interval corresponds to a frequency of  $2.77 \times 10^{-3} \text{ d}^{-1}$  (vertical line, purple on-line). It corresponds to a period of  $\simeq 1$  year. The shaded (green on-line) area – calculated by Monte Carlo procedure – represents the 90% C.L. region where all the peaks are expected to fall for the (1–6) keV energy interval.

In the case below 6 keV, a signal is present; thus, to properly evaluate the C.L. the signal must be included. This has been done by a dedicated Monte Carlo procedure where a large number of similar experiments has been simulated. The 90% C.L. region (shaded, green on-line) where all the peaks are expected to fall for the (2–6) keV energy interval is reported in Fig 6. Several peaks, satellite of the one year period frequency, are present.

In conclusion, apart from the peak corresponding to a 1 year period, no other peak is statistically significant either in the low and high energy regions.

Moreover, for each annual cycle of DAMA/LIBRA–phase1 and phase2, the annual baseline counting rates have been calculated for the (2–6) keV energy interval. Their power spectrum in the frequency range  $0.00013 - 0.0019 \text{ d}^{-1}$  (correspond-

ing to a period range 1.4–21.1 year) has been calculated according to Ref.<sup>5</sup>. No statistically-significant peak is present at frequencies lower than  $1 \text{ yr}^{-1}$ . This implies that no evidence for a long term modulation in the counting rate is present.

Finally, the case of the (1–6) keV energy interval of the DAMA/LIBRA–phase2 data is reported in Fig. 7. As previously the only significant peak is the one corresponding to one year period. No other peak is statistically significant being below the shaded (green on-line) area obtained by Monte Carlo procedure.

## 6. The modulation amplitudes by the maximum likelihood approach

The annual modulation present at low energy can also be pointed out by depicting the energy dependence of the modulation amplitude,  $S_m(E)$ , obtained by maximum likelihood method considering fixed period and phase:  $T = 1 \text{ yr}$  and  $t_0 = 152.5 \text{ day}$ . For such purpose the likelihood function of the *single-hit* experimental data in the  $k$ -th energy bin is defined as:  $\mathbf{L}_k = \prod_{ij} e^{-\mu_{ijk}} \frac{\mu_{ijk}^{N_{ijk}}}{N_{ijk}!}$ , where  $N_{ijk}$  is the number of events collected in the  $i$ -th time interval (hereafter 1 day), by the  $j$ -th detector and in the  $k$ -th energy bin.  $N_{ijk}$  follows a Poisson's distribution with expectation value  $\mu_{ijk} = [b_{jk} + S_i(E_k)] M_j \Delta t_i \Delta E \epsilon_{jk}$ . The  $b_{jk}$  are the background contributions,  $M_j$  is the mass of the  $j$ -th detector,  $\Delta t_i$  is the detector running time during the  $i$ -th time interval,  $\Delta E$  is the chosen energy bin,  $\epsilon_{jk}$  is the overall efficiency. The signal can be written as:

$$S_i(E) = S_0(E) + S_m(E) \cdot \cos \omega(t_i - t_0),$$

where  $S_0(E)$  is the constant part of the signal and  $S_m(E)$  is the modulation amplitude. The usual procedure is to minimize the function  $y_k = -2 \ln(\mathbf{L}_k) - \text{const}$  for each energy bin; the free parameters of the fit are the  $(b_{jk} + S_0)$  contributions and the  $S_m$  parameter.

The modulation amplitudes for the whole data sets: DAMA/NaI, DAMA/LIBRA–phase1 and DAMA/LIBRA–phase2 (total exposure 2.86 ton×yr) are plotted in Fig. 8; the data below 2 keV refer only to the DAMA/LIBRA–phase2 exposure (1.53 ton×yr). It can be inferred that positive signal is present in the (1–6) keV energy interval, while  $S_m$  values compatible with zero are present just above. All this confirms the previous analyses. The test of the hypothesis that the  $S_m$  values in the (6–14) keV energy interval have random fluctuations around zero yields  $\chi^2/d.o.f.$  equal to 20.3/16 (P-value = 21%).

For the case of (6–20) keV energy interval  $\chi^2/d.o.f. = 42.2/28$  (P-value = 4%). The obtained  $\chi^2$  value is rather large due mainly to two data points, whose centroids are at 16.75 and 18.25 keV, far away from the (1–6) keV energy interval. The P-values obtained by excluding only the first and either the points are 14% and 23%.

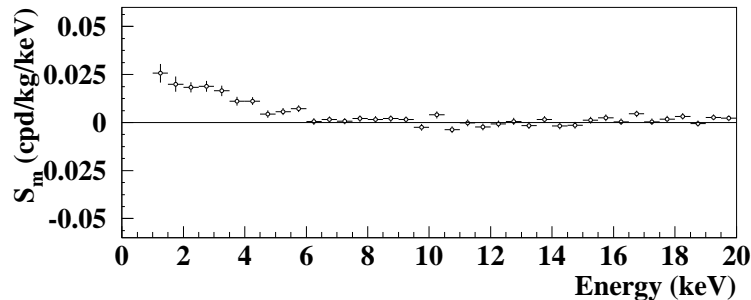


Fig. 8. Modulation amplitudes,  $S_m$ , for the whole data sets: DAMA/NaI, DAMA/LIBRA-phase1 and DAMA/LIBRA-phase2 (total exposure  $2.86 \text{ ton} \times \text{yr}$ ) above 2 keV; below 2 keV only the DAMA/LIBRA-phase2 exposure ( $1.53 \text{ ton} \times \text{yr}$ ) is available and used. The energy bin  $\Delta E$  is 0.5 keV. A clear modulation is present in the lowest energy region, while  $S_m$  values compatible with zero are present just above. In fact, the  $S_m$  values in the (6–20) keV energy interval have random fluctuations around zero with  $\chi^2/d.o.f.$  equal to  $42.2/28$  (P-value is 4%).

### 6.1. The $S_m$ distributions

The method also allows the extraction of the  $S_m$  values for each detector. In particular, the modulation amplitudes  $S_m$  integrated in the range (2–6) keV for each of the 25 detectors for the DAMA/LIBRA-phase1 and DAMA/LIBRA-phase2 periods can be produced. They have random fluctuations around the weighted averaged value confirmed by the  $\chi^2$  analysis. Thus, the hypothesis that the signal is well distributed over all the 25 detectors is accepted.

As previously done for the other data releases<sup>2-5,19-21,23</sup>, the  $S_m$  values for each detector for each annual cycle and for each energy bin have been obtained. The  $S_m$  are expected to follow a normal distribution in absence of any systematic effects. Therefore, the variable  $x = \frac{S_m - \langle S_m \rangle}{\sigma}$  has been considered to verify that the  $S_m$  are statistically well distributed in the 16 energy bins ( $\Delta E = 0.25$  keV) in the (2–6) keV energy interval of the seven DAMA/LIBRA-phase1 annual cycles and in the 20 energy bins in the (1–6) keV energy interval of the eight DAMA/LIBRA-phase2 annual cycles and in each detector. Here,  $\sigma$  are the errors associated to  $S_m$  and  $\langle S_m \rangle$  are the mean values of the  $S_m$  averaged over the detectors and the annual cycles for each considered energy bin.

Defining  $\chi^2 = \sum x^2$ , where the sum is extended over all the 272 (192 for the 16<sup>th</sup> detector<sup>4</sup>)  $x$  values,  $\chi^2/d.o.f.$  values ranging from 0.8 to 2.0 are obtained, depending on the detector.

The mean value of the 25  $\chi^2/d.o.f.$  is 1.092, slightly larger than 1. Although this can be still ascribed to statistical fluctuations, let us ascribe it to a possible systematic. In this case, one would derive an additional error to the modulation amplitude measured below 6 keV:  $\leq 2.4 \times 10^{-4}$  cpd/kg/keV, if combining quadratically the errors, or  $\leq 3.6 \times 10^{-5}$  cpd/kg/keV, if linearly combining them. This possible

additional error:  $\leq 2.4\%$  or  $\leq 0.4\%$ , respectively, on the DAMA/LIBRA-phase1 and DAMA/LIBRA-phase2 modulation amplitudes is an upper limit of possible systematic effects coming from the detector to detector differences.

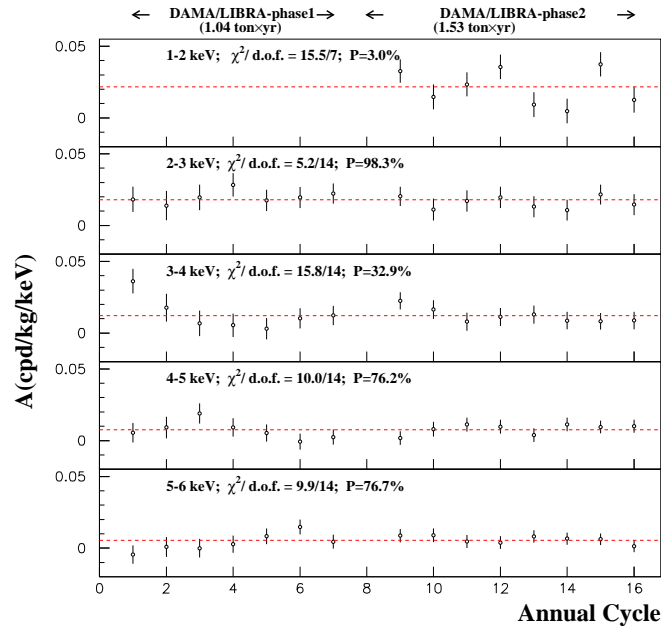


Fig. 9. Modulation amplitudes of each single annual cycle of DAMA/LIBRA-phase1 and DAMA/LIBRA-phase2. The error bars are the  $1\sigma$  errors. The dashed horizontal lines show the central values obtained by best fit over the whole data set. The  $\chi^2$  test and the *run test* accept the hypothesis at 95% C.L. that the modulation amplitudes are normally fluctuating around the best fit values.

Among further additional tests, the analysis of the modulation amplitudes as a function of the energy separately for the nine inner detectors and the remaining external ones has been carried out for DAMA/LIBRA-phase1 and DAMA/LIBRA-phase2, as already done for the other data sets<sup>2-5,19-21,23</sup>. The obtained values are fully in agreement; in fact, the hypothesis that the two sets of modulation amplitudes belong to same distribution has been verified by  $\chi^2$  test, obtaining e.g.:  $\chi^2/d.o.f. = 1.9/6$  and  $36.1/38$  for the energy intervals (1-4) and (1-20) keV, respectively ( $\Delta E = 0.5$  keV). This shows that the effect is also well shared between inner and outer detectors.

Fig. 9 shows the modulation amplitudes singularly calculated for each annual cycle of DAMA/LIBRA-phase1 and DAMA/LIBRA-phase2. To test the hypothesis that the amplitudes are compatible and normally fluctuating around their mean values, the  $\chi^2$  test has been performed. The  $\chi^2/d.o.f.$  values and the P-values are also shown in Fig. 9. In addition to the  $\chi^2$  test, another independent statistical test has been applied: the *run test* (see e.g. Ref.<sup>69</sup>); it verifies the hypothesis that the

positive (above the mean value) and negative (under the mean value) data points are randomly distributed. The lower (upper) tail probabilities obtained by the *run test* are: 89(37)%, 87(30)%, 17(94)%, 17(94)% and 30(85)%, respectively. This analysis confirms that the data collected in all the annual cycles with DAMA/LIBRA–phase1 and phase2 are statistically compatible and can be considered together.

## 7. Investigation of the annual modulation phase

Let us, finally, release the assumption of the phase  $t_0 = 152.5$  day in the procedure to evaluate the modulation amplitudes. In this case the signal can be alternatively written as:

$$\begin{aligned} S_i(E) &= S_0(E) + S_m(E) \cos \omega(t_i - t_0) + Z_m(E) \sin \omega(t_i - t_0) \\ &= S_0(E) + Y_m(E) \cos \omega(t_i - t^*). \end{aligned} \quad (1)$$

For signals induced by DM particles one should expect: i)  $Z_m \sim 0$  (because of the orthogonality between the cosine and the sine functions); ii)  $S_m \simeq Y_m$ ; iii)  $t^* \simeq t_0 = 152.5$  day. In fact, these conditions hold for most of the dark halo models; however, as mentioned above, slight differences can be expected in case of possible contributions from non-thermalized DM components (see e.g. Refs.<sup>38,58,59,61–63</sup>).

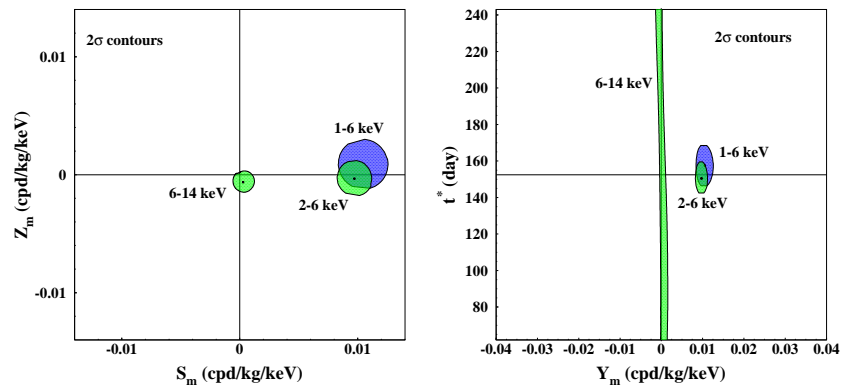


Fig. 10.  $2\sigma$  contours in the plane  $(S_m, Z_m)$  (left) and in the plane  $(Y_m, t^*)$  (right) for: i) DAMA/NaI, DAMA/LIBRA–phase1 and DAMA/LIBRA–phase2 in the (2–6) keV and (6–14) keV energy intervals (light areas, green on-line); ii) only DAMA/LIBRA–phase2 in the (1–6) keV energy interval (dark areas, blue on-line). The contours have been obtained by the maximum likelihood method. A modulation amplitude is present in the lower energy intervals and the phase agrees with that expected for DM induced signals.

Considering cumulatively the data of DAMA/NaI, DAMA/LIBRA–phase1 and DAMA/LIBRA–phase2 the obtained  $2\sigma$  contours in the plane  $(S_m, Z_m)$  for the (2–6) keV and (6–14) keV energy intervals are shown in Fig. 10–left while in Fig. 10–right the obtained  $2\sigma$  contours in the plane  $(Y_m, t^*)$  are depicted. Moreover, Fig. 10 also shows only for DAMA/LIBRA–phase2 the  $2\sigma$  contours in the (1–6) keV energy interval.



The best fit values in the considered cases ( $1\sigma$  errors) for  $S_m$  versus  $Z_m$  and  $Y_m$  versus  $t^*$  are reported in Table 4.

Table 4. Best fit values ( $1\sigma$  errors) for  $S_m$  versus  $Z_m$  and  $Y_m$  versus  $t^*$ , considering: i) DAMA/NaI, DAMA/LIBRA-phase1 and DAMA/LIBRA-phase2 in the (2–6) keV and (6–14) keV energy intervals; ii) only DAMA/LIBRA-phase2 in the (1–6) keV energy interval. See also Fig. 10.

E (keV)	$S_m$ (cpd/kg/keV)	$Z_m$ (cpd/kg/keV)	$Y_m$ (cpd/kg/keV)	$t^*$ (day)
DAMA/NaI+DAMA/LIBRA-phase1+DAMA/LIBRA-phase2:				
2–6	$(0.0097 \pm 0.0007)$	$-(0.0003 \pm 0.0007)$	$(0.0097 \pm 0.0007)$	$(150.5 \pm 4.0)$
6–14	$(0.0003 \pm 0.0005)$	$-(0.0006 \pm 0.0005)$	$(0.0007 \pm 0.0010)$	undefined
DAMA/LIBRA-phase2:				
1–6	$(0.0104 \pm 0.0007)$	$(0.0002 \pm 0.0007)$	$(0.0104 \pm 0.0007)$	$(153.5 \pm 4.0)$

Finally, setting  $S_m$  in eq. (1) to zero, the  $Z_m$  values as function of the energy have also been determined by using the same procedure. The  $Z_m$  values as a function of the energy for DAMA/NaI, DAMA/LIBRA-phase1, and DAMA/LIBRA-phase2 data sets are expected to be zero. The  $\chi^2$  test applied to the data supports the hypothesis that the  $Z_m$  values are simply fluctuating around zero; in fact, in the (1–20) keV energy region the  $\chi^2/d.o.f.$  is equal to 40.6/38 corresponding to a P-value = 36%.

The energy behaviors of the  $Y_m$  and of the phase  $t^*$  are produced for the cumulative exposure of DAMA/NaI, DAMA/LIBRA-phase1, and DAMA/LIBRA-phase2. As in the previous analyses, an annual modulation effect is present in the lower energy intervals and the phase agrees with that expected for DM induced signals. No modulation is present above 6 keV and the phase is undetermined.

## 8. Perspectives

To further increase the experimental sensitivity of DAMA/LIBRA and to disentangle some of the many possible astrophysical, nuclear and particle physics scenarios in the investigation on the DM candidate particle(s), an increase of the exposure in the lowest energy bin and a further decreasing of the software energy threshold are needed. This is pursued by running DAMA/LIBRA-phase2 and upgrading the experimental set-up to lower the software energy threshold below 1 keV with high acceptance efficiency.

Firstly, particular efforts for lowering the software energy threshold have been done in the already-acquired data of DAMA/LIBRA-phase2 by using the same technique as before with dedicated studies on the efficiency. As consequence, a new data point has been added in the modulation amplitude as function of energy down to 0.75 keV, see Fig. 11. A modulation is also present below 1 keV, from 0.75 keV. This preliminary result confirms the necessity to lower the software energy threshold

by a hardware upgrade and an improved statistics in the first energy bin.

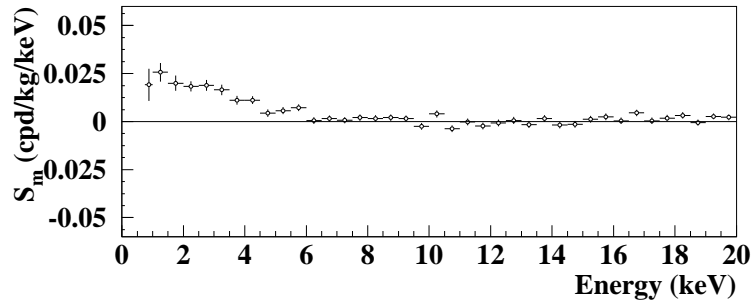


Fig. 11. As Fig. 8; the new data point below 1 keV, with software energy threshold at 0.75 keV, shows that an annual modulation is also present below 1 keV. This preliminary result confirms the necessity to lower the software energy threshold by a hardware upgrade and to improve the experimental error on the first energy bin.

This dedicated hardware upgrade of DAMA/LIBRA-phase2 is underway. It consists in equipping all the PMTs with miniaturized low background new concept preamplifier and HV divider mounted on the same socket, and related improvements of the electronic chain, mainly the use of higher vertical resolution 14-bit digitizers.

## 9. Conclusions

DAMA/LIBRA-phase2 confirms a peculiar annual modulation of the *single-hit* scintillation events in the (1–6) keV energy region satisfying all the many requirements of the DM annual modulation signature; the cumulative exposure by the former DAMA/NaI, DAMA/LIBRA-phase1 and DAMA/LIBRA-phase2 is 2.86 ton  $\times$  yr.

As required by the exploited DM annual modulation signature: 1) the *single-hit* events show a clear cosine-like modulation as expected for the DM signal; 2) the measured period is well compatible with the 1 yr period as expected for the DM signal; 3) the measured phase is compatible with the roughly  $\simeq 152.5$  days expected for the DM signal; 4) the modulation is present only in the low energy (1–6) keV interval and not in other higher energy regions, consistently with expectation for the DM signal; 5) the modulation is present only in the *single-hit* events, while it is absent in the *multiple-hit* ones as expected for the DM signal; 6) the measured modulation amplitude in NaI(Tl) target of the *single-hit* scintillation events in the (2–6) keV energy interval, for which data are also available by DAMA/NaI and DAMA/LIBRA-phase1, is:  $(0.01014 \pm 0.00074)$  cpd/kg/keV ( $13.7 \sigma$  C.L.). No systematic or side processes able to mimic the signature, i.e. able to simultaneously satisfy all the many peculiarities of the signature and to account for the whole measured modulation amplitude, has been found or suggested by anyone throughout some decades thus far. In particular, arguments related to any possible role of some natural periodical phenomena have been discussed and quantitatively demonstrated

to be unable to mimic the signature (see references; e.g. Refs.<sup>7,8</sup>). Thus, on the basis of the exploited signature, the model independent DAMA results give evidence at  $13.7\sigma$  C.L. (over 22 independent annual cycles and in various experimental configurations) for the presence of DM particles in the galactic halo.

The new data, released in this Conference, determine the modulation parameters with increasing precision and allow us to disentangle with larger C.L. among different DM candidates, DM models and astrophysical, nuclear and particle physics scenarios.

The DAMA model independent evidence is compatible with a wide set of astrophysical, nuclear and particle physics scenarios for high and low mass candidates inducing nuclear recoil and/or electromagnetic radiation, as also shown in various literature. Moreover, both the negative results and all the possible positive hints, achieved so-far in the field, can be compatible with the DAMA model independent DM annual modulation results in many scenarios considering also the existing experimental and theoretical uncertainties; the same holds for indirect approaches. For a discussion see e.g. Ref.<sup>5</sup> and references therein.

Finally, we stress that to efficiently disentangle among at least some of the many possible candidates and scenarios an increase of exposure in the new lowest energy bin and the decrease of the software energy threshold below the present 1 keV is important. The experiment is collecting data and the hardware efforts towards the lowering of the software energy threshold is in progress.

## References

1. R. Bernabei et al., *Nucl. Instr. and Meth. A* **592**, 297 (2008).
2. R. Bernabei et al., *Eur. Phys. J. C* **56**, 333 (2008).
3. R. Bernabei et al., *Eur. Phys. J. C* **67**, 39 (2010).
4. R. Bernabei et al., *Eur. Phys. J. C* **73**, 2648 (2013).
5. R. Bernabei et al., *Int. J. of Mod. Phys. A* **28**, 1330022 (2013).
6. R. Bernabei et al., *J. of Instr.* **7**, P03009 (2012).
7. R. Bernabei et al., *Eur. Phys. J. C* **72**, 2064 (2012).
8. R. Bernabei et al., *Eur. Phys. J. C* **74**, 3196 (2014).
9. DAMA coll., issue dedicated to DAMA, *Int. J. of Mod. Phys. A* **31** (2016) and refs therein.
10. R. Bernabei et al., *Eur. Phys. J. C* **74**, 2827 (2014).
11. R. Bernabei et al., *Eur. Phys. J. C* **62**, 327 (2009).
12. R. Bernabei et al., *Eur. Phys. J. C* **72**, 1920 (2012).
13. R. Bernabei et al., *Eur. Phys. J. A* **49**, 64 (2013).
14. R. Bernabei et al., *Eur. Phys. J. C* **75**, 239 (2015).
15. P. Belli et al., *Phys. Rev. D* **84**, 055014 (2011).
16. A. Addazi et al., *Eur. Phys. J. C* **75**, 400 (2015).
17. R. Bernabei et al., *Int. J. of Mod. Phys. A* **31**, 1642009 (2016).
18. R. Cerulli et al., *Eur. Phys. J. C* **77**, 83 (2017).
19. R. Bernabei et al., *Universe* **4**, 116 (2018).
20. R. Bernabei et al., *Nucl. Phys. At. Energy* **19**, 307 (2018).
21. R. Bernabei, *Bled Workshops in Physics* **19** n. 2, 27 (2018).
22. R. Bernabei et al., *Nucl. Phys. At. Energy* **20(4)**, 317 (2019).

23. R. Bernabei et al., *Prog. Part. Nucl. Phys.* **114**, 103810 (2020).
24. P. Belli, R. Bernabei, C. Bacci, A. Incicchitti, R. Marcovaldi, D. Prosperi, DAMA proposal to INFN Scientific Committee II, April 24<sup>th</sup> 1990.
25. R. Bernabei et al., *Phys. Lett. B* **389**, 757 (1996).
26. R. Bernabei et al., *Phys. Lett. B* **424**, 195 (1998).
27. R. Bernabei et al., *Phys. Lett. B* **450**, 448 (1999).
28. P. Belli et al., *Phys. Rev. D* **61**, 023512 (2000).
29. R. Bernabei et al., *Phys. Lett. B* **480**, 23 (2000).
30. R. Bernabei et al., *Phys. Lett. B* **509**, 197 (2001).
31. R. Bernabei et al., *Eur. Phys. J. C* **23**, 61 (2002).
32. P. Belli et al., *Phys. Rev. D* **66**, 043503 (2002).
33. R. Bernabei et al., *Il Nuovo Cim. A* **112**, 545 (1999).
34. R. Bernabei et al., *Eur. Phys. J. C* **18**, 283 (2000).
35. R. Bernabei et al., *La Rivista del Nuovo Cimento* **26** n.1, 1-73 (2003), and refs. therein.
36. R. Bernabei et al., *Int. J. Mod. Phys. D* **13**, 2127 (2004) and refs. therein.
37. R. Bernabei et al., *Int. J. Mod. Phys. A* **21**, 1445 (2006).
38. R. Bernabei et al., *Eur. Phys. J. C* **47**, 263 (2006).
39. R. Bernabei et al., *Int. J. Mod. Phys. A* **22**, 3155 (2007).
40. R. Bernabei et al., *Eur. Phys. J. C* **53**, 205 (2008).
41. R. Bernabei et al., *Phys. Rev. D* **77**, 023506 (2008).
42. R. Bernabei et al., *Mod. Phys. Lett. A* **23**, 2125 (2008).
43. R. Bernabei et al., *Phys. Lett. B* **408**, 439 (1997).
44. P. Belli et al., *Phys. Lett. B* **460**, 236 (1999).
45. R. Bernabei et al., *Phys. Rev. Lett.* **83**, 4918 (1999).
46. P. Belli et al., *Phys. Rev. C* **60**, 065501 (1999).
47. R. Bernabei et al., *Il Nuovo Cimento A* **112**, 1541 (1999).
48. R. Bernabei et al., *Phys. Lett. B* **515**, 6 (2001).
49. F. Cappella et al., *Eur. Phys. J.-direct C* **14**, 1 (2002).
50. R. Bernabei et al., *Eur. Phys. J. A* **23**, 7 (2005).
51. R. Bernabei et al., *Eur. Phys. J. A* **24**, 51 (2005).
52. K.A. Drukier et al., *Phys. Rev. D* **33**, 3495 (1986).
53. K. Freese et al., *Phys. Rev. D* **37**, 3388 (1988).
54. R. Bernabei and A. Incicchitti, *Int. J. Mod. Phys. A* **32**, 1743007 (2017).
55. D. Smith and N. Weiner, *Phys. Rev. D* **64**, 043502 (2001).
56. D. Tucker-Smith and N. Weiner, *Phys. Rev. D* **72**, 063509 (2005).
57. D. P. Finkbeiner et al., *Phys. Rev. D* **80**, 115008 (2009).
58. K. Freese et al., *Phys. Rev. D* **71**, 043516 (2005).
59. K. Freese et al., *Phys. Rev. Lett.* **92**, 111301 (2004).
60. P. Belli et al., *Int. J. of Mod. Phys. A* **31**, 1642005 (2016).
61. P. Gondolo et al., *New Astron. Rev.* **49**, 193 (2005).
62. G. Gelmini and P. Gondolo, *Phys. Rev. D* **64**, 023504 (2001).
63. F.S. Ling, P. Sikivie and S. Wick, *Phys. Rev. D* **70**, 123503 (2004).
64. G. Ranucci and M. Rovere, *Phys. Rev. D* **75**, 013010 (2007).
65. J.D. Scargle, *Astrophys. J.* **263**, 835 (1982).
66. W.H. Press et al., *Numerical recipes in Fortran 77: the art of scientific computing*, Cambridge University Press, Cambridge, England 1992, section 13.8.
67. J.H. Horne and S.L. Baliunas, *Astrophys. J.* **302**, 757 (1986).
68. R. Bernabei et al., *Bled Workshop in Physics* **15**, no. 2, 19 (2014).
69. W.T. Eadie et al., *Statistical methods in experimental physics*, ed. American Elsevier Pub. (1971).